![The University of Edinburgh logo]

Edinburgh Research Explorer

Optimization of Nafion Polymer Electrolyte Membrane Design and Microfabrication

OPEN ACCESS

Optimization of Nafion Polymer Electrolyte Membrane Design and Microfabrication

Jamie R.K. Marland, Fiona Moore, Camelia Dunare, Andreas Tsiamis, Eva González-Fernández,
Ewen O. Blair, Stewart Smith *Senior Member, IEEE*, Jonathan G. Terry, *Senior Member, IEEE*,
Alan F. Murray, *Fellow, IEEE*, Anthony J. Walton, *Senior Member, IEEE*

Abstract — **Nafion is a solid electrolyte polymer that can be used as a sensor membrane in microfabricated electrochemical oxygen sensors. It allows ions to be transported between the sensor electrodes and removes the need for a liquid electrolyte. Here we used a series of small square Nafion test structures, fabricated on a variety of materials using standard thin-film patterning techniques, to optimize the design and processing of Nafion membranes. Measurements showed that the choice of photoresist developer is critical. Use of diluted MF-26A developer provided the most effective and manufacturable process. The underlying material also had an influence on robustness, with silicon dioxide and platinum giving the longest membrane lifetime under simulated conditions of use. Membrane size had no clear effect on lifetime, and under optimal processing conditions there were minimal failures even under continuous mechanical agitation for up to six weeks. We also developed test electrodes covered by Nafion, and showed that they were effective at supporting electrochemical oxygen detection.**

Index Terms — **Biomedical monitoring, Electrochemical devices, Membranes, Micromachining, Oxygen, Thin film devices, Microsensors**

I. INTRODUCTION

DEVELOPMENT of active implantable medical devices containing electronic sensors is a focus of much current attention. Tissue oxygenation monitoring is a particularly valuable sensor modality, as it is likely to be useful for a wide range of clinical applications. These include cancer radiotherapy where tumor hypoxia leads to treatment resistance [1], management of traumatic brain injury [2], and in post-surgical and critical care [3]. A key challenge in creating sensors suitable for implantation is minimizing their size and dependence on external instrumentation. Manufacturing sensors using semiconductor microfabrication techniques presents an opportunity to meet these challenges through miniaturization, reduced power consumption, and the potential of integration with CMOS circuits for signal processing and wireless operation.

However, sensor microfabrication often involves the use of non-standard materials and novel processes to create devices with the necessary functionality that can operate in a biological environment. New methods for optimizing sensor manufacture on silicon wafers are therefore required.

Sensor based oxygen detection technologies fall into two main groups: optical measurement using phosphorescence of oxygen-sensitive compounds, and direct electrochemical measurement using electrodes [4]. Here we present a series of test structure measurements that were used in the development of a miniature implantable "Clark electrode" electrochemical oxygen sensor. A Clark electrode with a membrane-covered cavity containing a liquid electrolyte is a well-established oxygen sensor for physiological monitoring [5]. Oxygen is measured electrochemically at a working electrode, producing an electrical current due to its reduction that is proportional to the local oxygen concentration:

$$O_2 + 4H^+ + 4e^- \rightarrow 2H_2O$$
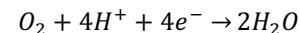
The standard Clark electrode architecture does not lend itself to miniaturization using standard microsystem technologies, due to its use of a liquid electrolyte. An alternative approach is to use the solid electrolyte Nafion. This is a polymer with ionic properties that contains hydrated channels capable of conducting protons [6]. It has been reported as a suitable electrolyte membrane in microfabricated electrochemical sensors that detect dissolved oxygen [7-10], indicating the feasibility of the approach.

These oxygen sensors have typically used drop-cast Nafion that is individually dispensed at die level. To mass-manufacture devices on silicon, an alternative wafer-level approach is needed. However, little has been reported about wafer-level microfabrication of Nafion membranes. To explore this issue quantitatively, we developed test structures to characterize and

J.R.K. Marland, F. Moore, C. Dunare, A. Tsiamis, S. Smith, J.G. Terry, A.F. Murray & A.J. Walton are with the School of Engineering, The University of Edinburgh, Alexander Crum Brown Road, Edinburgh, EH9 3FF, UK (Email: jamie.marland@ed.ac.uk). E. González-Fernández is with the School of Chemistry, The University of Edinburgh, Joseph Black Building, Edinburgh, EH9 3FJ, UK. E.O. Blair is with the Department of Biomedical Engineering, University of Strathclyde, Glasgow, G4 0NS, UK.
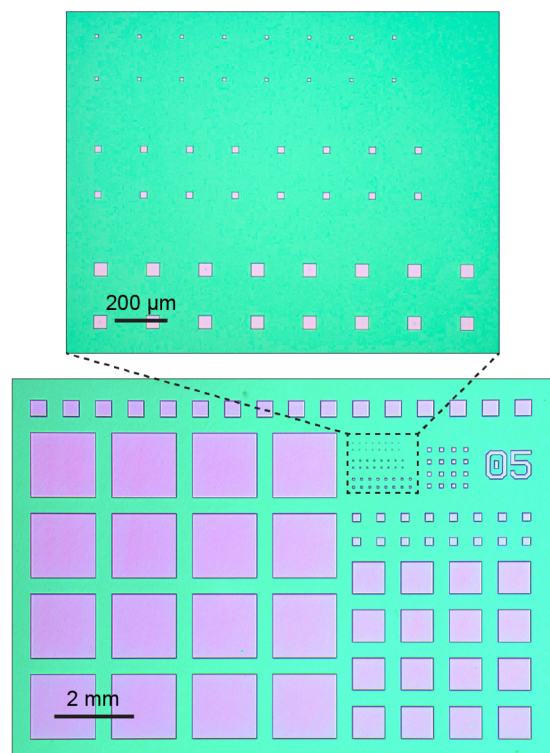
Fig. 1. Test structure layout for investigating Nafion membrane fabrication parameters. Example optical images of fabricated layout block containing Nafion squares with widths between 1600 μm and 12.5 μm. All feature sizes were fully resolved. These images show Nafion membranes on LFSIO.
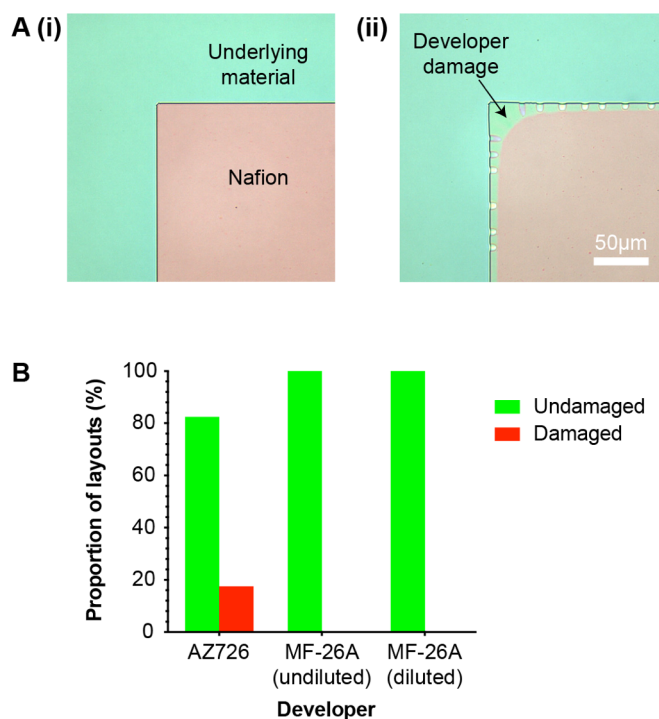

Fig. 2. Photoresist developer damage to Nafion test structures. A: Example images showing corners of patterned Nafion test structures that were visibly either (i) undamaged, or (ii) damaged by photoresist developer during processing. These image shows Nafion membranes on LFSIO. B: Proportion of layouts damaged by different developers; n ≥ 120 layouts from 5 wafers for each developer.

optimize the design and patterning of Nafion membranes. A set of test electrodes was also fabricated to demonstrate the ability of a microfabricated Nafion layer to support electrochemical reactions.

The concept of these test structures, and principle data demonstrating their use, were previously reported in a conference paper for the 2017 IEEE International Conference on Microelectronic Test Structures [11]. Here we present a refined version of the test structures, and describe expanded results including further process optimization and structure testing.

II. NAFION ADHESION AND DURABILITY TEST STRUCTURES

A. Design

Layouts containing simple square test structures were designed for optimizing the fabrication process, and investigating the effects of membrane dimensions and underlying materials on Nafion adhesion and durability. Layouts contained multiple instances of squares with widths ranging from 1600 μm to 12.5 μm (shown in Fig. 1), or a very similar design containing a more limited width range of 1600 μm − 200 μm (described previously [11]). The layouts were designed within blocks, with a total of 12 or 18 blocks evenly distributed across the surface of a 100 mm diameter silicon wafer.

B. Fabrication

To fabricate the test structures, materials that would potentially be used for either the sensor electrodes (platinum), or the top dielectric layer, were deposited on silicon wafers. The top dielectric was formed by plasma enhanced chemical vapor deposition (PECVD) of low-frequency/high-frequency silicon nitride (LFSIN/HFSIN), or silicon dioxide (LFSIO/HFSIO). The wafers were treated with a Silane A-174 adhesion promoter solution [10], and spin-coated at 500 rpm with a Nafion solution (5% Nafion in lower aliphatic alcohols and water, Sigma-Aldrich cat. #274704), then dried in air at room temperature and thermally annealed to improve solvent resistance [12]. Spin coating is a straightforward, versatile, and reproducible technique for fabricating polymer thin films from solution. Film thickness can be controlled by changing spin speed and solution concentration [13], although here we used a fixed set of conditions to allow valid comparisons to be made between different membrane designs or underlying materials. Wafers were then spin-coated in SPR350 photoresist, and the test structure patterns transferred into photoresist by photolithography (Karl Suss MA8). Three different processes for photoresist development were trialed, using developers compatible with SPR350 photoresist. Off-the-shelf (undiluted) MF-26A or AZ726 developer were used for 10 s, followed by rinsing in deionized water, repeated until the resist was fully developed (typically 30 − 40 s development in total). A solution of MF-26A diluted 2:1 (developer : deionized water) was also
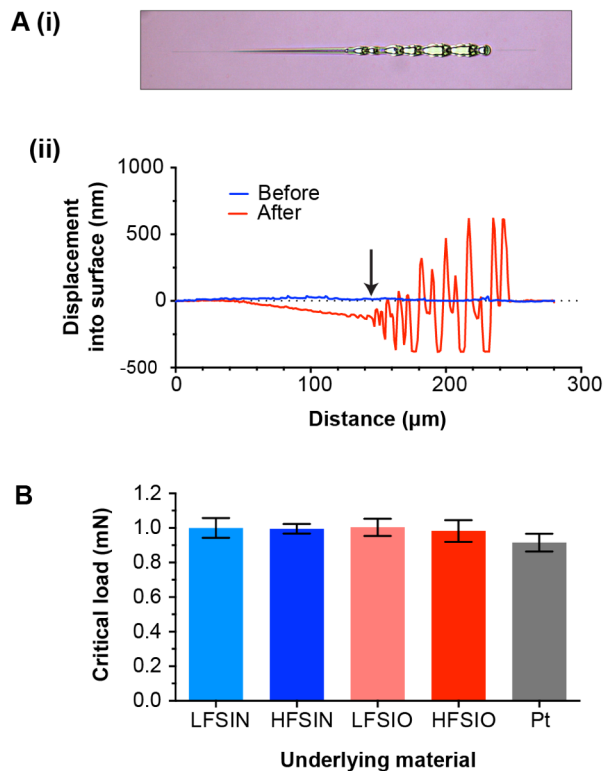
A (i)

(ii)

Fig. 3. Scratch tests to measure Nafion adhesion. A: (i) Representative image of a scratch made through a Nafion layer, and (ii) representative profilometry trace showing surface profile before and after scratch, arrow indicates critical load. B: Quantification of critical loads for Nafion on different underlying materials; n = 4 locations/material, 10 scratches at each location, error bars show standard error of the mean.
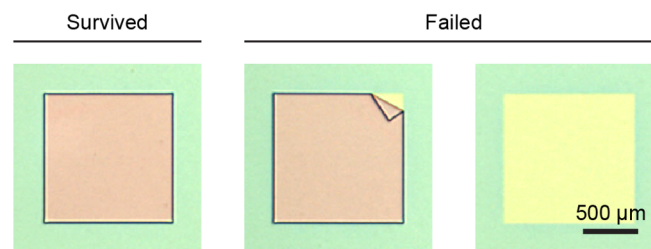

Fig. 4. Example images showing survival and failure of Nafion test structures following immersion in PBS. Visible outlines of the structures remaining after failure are due to over-etching or roughening of the wafer material outside the Nafion structure during etching.

tested, using a 90 s development without wash intervals. Nafion was then patterned by reactive ion plasma etching. Photoresist was stripped off using an acetone wet stripping process prior to testing. Profilometry measurements of Nafion features gave a mean thickness of 0.42 ± 0.08 μm across the fabricated wafers (n = 20 wafers).

Optical inspection of the test structures on wafers processed using AZ726 photoresist developer indicated that some displayed damage to their edges suggesting delamination, while wafers processed using either diluted or undiluted MF-26A developer were all intact and undamaged (Fig. 2). MF-26A and AZ726 developers are both based on an alkaline aqueous solution of tetramethylammonium hydroxide (TMAH). However, as they have an identical TMAH concentration of 0.26 N, it is likely that different proprietary additives such as surfactants present in the developers may be responsible for their differing compatibility profiles. Diluting MF-26A further improved the process, as no damage occurred even at the extended development time used here. Multiple inspection steps to prevent over-development and Nafion damage were not required, maximizing manufacturability.

III. ADHESION MEASUREMENTS

Nafion adhesion strength on the different materials was measured using a scratch tester (Keysight Nanoindenter G220). This tool draws a sharp tip across the surface of the layer under test with a ramped increase in downward force. The tip force when the layer fails is defined as the critical load. Magnitude of the critical load scales with adhesion strength between the layer under test and the underlying material, while the exact failure mode is affected by the hardness of the coating and substrate [14]. In this case with a soft coating and hard substrate, the expected failure mode is plastic deformation followed by interface failure [15]. Two selected locations on each wafer were measured, and for each test location an array of 10 scratches was performed.

Optical inspection of the scratches made in Nafion showed that, as expected, it underwent initial plastic deformation, followed by buckling and failure of the layer as it became detached from the wafer (Fig. 3A(i)). Profilometry was used to inspect the scratch location before and after testing in order to identify the exact failure point, and this showed a similar pattern (Fig. 3A(ii)). Due to the softness of the Nafion, there was also minor plastic deformation of the layer during the profilometry step, which accounts for the measured displacement after failure appearing to be slightly less than the expected layer thickness. Comparison of the scratch test results showed no significant differences in Nafion mean critical load between any conditions (Fig. 3B). This suggests that there were no differences between Nafion adhesion on any of the tested insulation layers, or on the conductive platinum layer.

IV. DURABILITY MEASUREMENTS

A. Incubation in PBS

To investigate whether any of the tested design parameters affected Nafion durability, test structure wafers were immersed in an aqueous phosphate buffered saline (PBS) solution, formulated to mimic the ionic composition of the body. Wafers were left in the solution for 6 weeks to simulate typical duration of use for the future oxygen sensor.
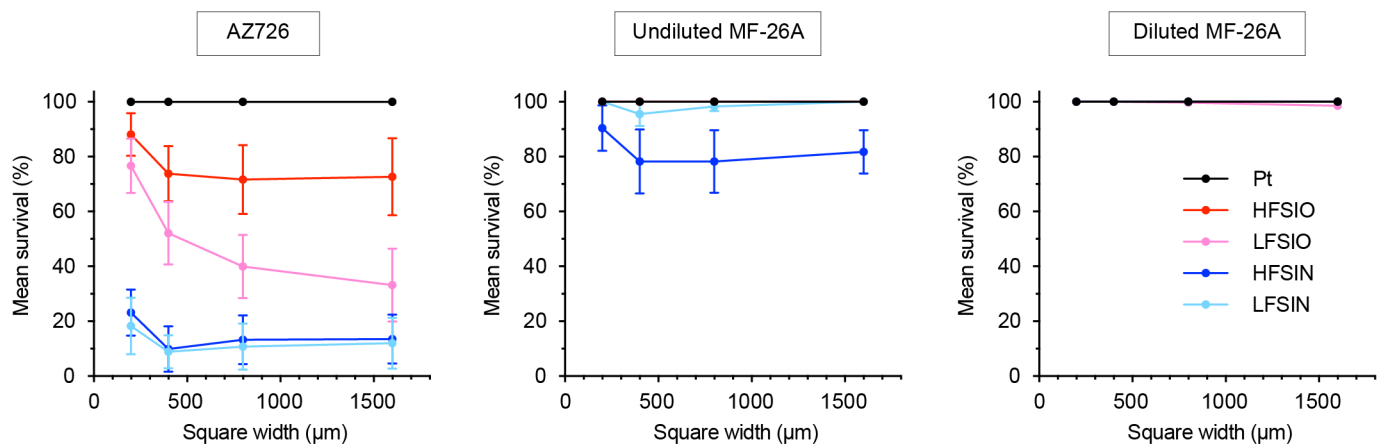
Fig. 5. Durability of Nafion test structures in PBS. Mean survival rates are shown for wafers processed in AZ726, MF-26A, or diluted MF-26A after immersion in PBS for 6 weeks. N ≥ 12 (insulators) or ≥ 6 (Pt) layouts for each condition, error bars indicate standard error of the mean.

As a measure of durability, survival of the test structures was evaluated by comparison of optical microscope images before and after immersion. A minimum of 6 instances of each test structure layout were tested for each combination of developer and underlying material. Structures were classified as having survived if they were undamaged at the end of the test, or failed if they were damaged or absent (Fig. 4).

There was a clear effect of the developer used during processing, with both sets of wafers processed using MF-26A showing higher overall survival, compared to those processed using AZ726 (Fig. 5). The difference in failure rate corresponds with the finding that damage to the Nafion edges (shown in Fig. 2) was far higher in wafers processed in AZ726. This suggests that the two effects may be linked, with damage during processing causing partial edge delamination that ultimately leads to failure of the structure during testing. However, despite no noticeable damage being found during the initial visual inspection, the wafers processed using undiluted MF-26A showed a lower survival than those processed using diluted MF-26A. This suggests that there could also be damage caused by the undiluted MF-26A to the Nafion structure which was not visible during inspection, but may have weakened the structure. Together, these results indicate that diluted MF-26A is optimal for Nafion processing in this application.

The underlying material also had a marked effect on structure survival and was particularly noticeable for the least optimal developers. The poorest survival was observed on wafers with PECVD silicon nitride surfaces. In contrast, structures fabricated on PECVD silicon dioxide surfaces showed intermediate survival on the wafers processed with AZ726, and near complete survival on wafers processed with MF-26A. This greater survival of structures on silicon dioxide may be attributable to the silane based adhesion promoter used during fabrication. It relies on a condensation reaction between an alkoxysilyl group in the adhesion promoter, and a hydroxyl

(-OH) group found on the wafer surface of hydrated silicon dioxide. Since few hydroxyl groups will be present on the silicon nitride, the adhesion promoter would be expected to perform less efficiently on this surface. The optimal PECVD deposition frequency appeared to be material specific, with better survival obtained for silicon nitride using low frequency deposition, and for silicon dioxide using high frequency deposition. Together these results show that use of PECVD high frequency silicon dioxide as an upper insulating layer is optimal for Nafion membrane durability in a sensor.

Interestingly, across all the materials tested, the best survival was obtained on platinum. This effect may be due to the known attractive interaction between platinum surfaces and the sulphonate groups in Nafion [16]. It provides reassurance that durability of the membrane will not be impaired by the presence of underlying platinum electrodes.

Nafion is known to swell in aqueous environments [6], which is likely to generate compressive stress within the layer that could lead to its failure. Such an effect is predicted to be strongest in larger structures with a greater area over which stress could build up. In keeping with this possibility, inspection of the structure survival data shows a trend towards increased survival of smaller sizes. However, this trend was weak and was absent under optimal processing conditions.

It is notable that the AZ726 and undiluted MF-26A survival results do not correlate with the adhesion measurements from scratch testing, which showed no differences between materials (Fig. 3). This suggests that the scratch test critical load of Nafion may not be usable as an indicator of its durability in PBS. The results do correlate with the survival results from wafers processed in diluted MF-26A, although it is possible that after a longer time these wafers may also begin to follow the trend shown by the wafers processed in undiluted developer.

B. Mechanical agitation

A more realistic and aggressive durability test was next performed using the test structures. The Nafion was processed using diluted MF-26A as the developer, since it was found to give optimal results. Wafers were immersed in a PBS solution for 6 weeks and agitated on an orbital shaking table at 125 rpm. This better simulates the movement and disturbance the sensor would be exposed to when implanted. Structures were again evaluated by optical microscopy, and survival or failure was classified as described previously.

The structures all showed near-complete survival after 6 weeks of agitation, with a survival rate ranging from $99.0 \pm 1.0\%$ to $100.0 \pm 0.0\%$ (mean $\pm$ SEM) across all the wafer substrates (Pt, HF/LFSIO, HF/LFSIN) and structure sizes (1600 – 12.5 µm) that were tested (n = 18 layouts for each substrate). There were no trends for the durability on different underlying materials or structure sizes. Again, it is possible that over longer time periods the survival results may still follow the trend established previously with the less optimal developers. These survival results match well with the survival results from the previous measurements using the diluted MF-26A. They show that the Nafion structures can withstand prolonged immersion and mechanical agitation, and support the ability of membranes fabricated in this way to survive when used as a solid electrolyte in an implantable oxygen sensor.

V. TEST ELECTRODES

A. Design

To function as an oxygen sensor electrolyte, the fabricated Nafion membrane must be both oxygen permeable and effectively support the electrochemical reduction of oxygen to water. To investigate these aspects of Nafion performance, a device containing test electrodes at which oxygen reduction could occur was designed and fabricated (Fig. 6A). The device was designed as a three-electrode electrochemical cell, with either a 50 or 125 µm wide square platinum working electrode (WE) at which the reaction of interest occurs. This is surrounded by a larger area platinum counter electrode (CE) to supply the necessary current to support the WE reaction. An additional electrode area for future use as an internal reference electrode (RE) was included on the device between the CE and WE, but not used in this study and left disconnected. Instead, an external commercial Ag/AgCl RE was used to ensure reference potential stability and minimise measurement variability.

B. Fabrication

The test electrodes were fabricated on thermally oxidized silicon wafers. Metal electrode surfaces and interconnect were formed from a 50 nm layer of platinum (with an underlying 10 nm titanium adhesion layer) deposited by e-beam
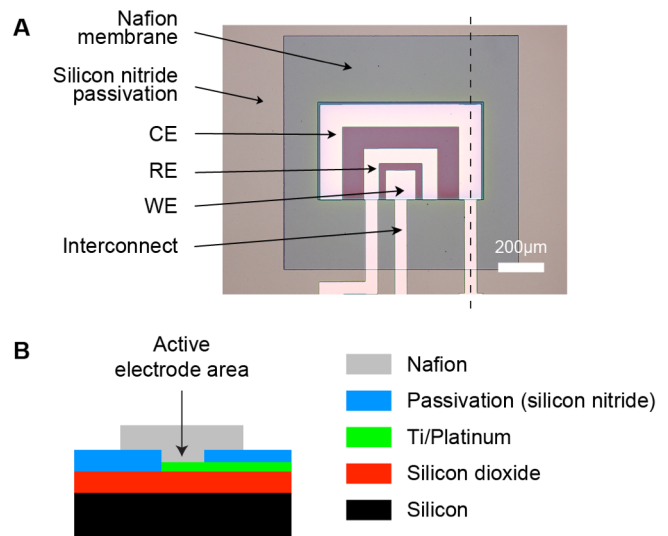

Fig. 6. Test electrode design and fabrication. A: Example image of fabricated test electrodes (125 µm WE device). Dashed line indicates location of cross-section drawing. B: Schematic cross-section of device architecture (not to scale).

evaporation, and patterned by lift-off processing. Aluminum was sputtered onto the wafer and patterned by lift-off processing to form contact pads. PECVD silicon nitride was deposited to insulate the metal interconnect, and patterned using RIE to produce windows permitting external access to the electrodes and contact pads. The electrodes were then either left bare, or covered in a square of Nafion deposited and patterned as before (Fig. 6B). Finally, the wafer was diced to enable each die to be tested separately.

C. Electrochemical testing

Nafion covered electrodes were tested in PBS, with the Nafion itself acting as the electrolyte, while the bare electrodes were bathed in 0.1 M KCl as a supporting electrolyte. The solutions were either saturated with air, or purged of oxygen using N_2, and the membrane and electrodes were tested by chronoamperometry over 20 s using a WE potential step (vs. Ag/AgCl) from +0.2 V (no oxygen reaction) to –0.7 V (oxygen reduction). All electrodes gave the expected profile of an initial transient current, followed by an approach to steady state (Fig. 7A). The current magnitudes were greater for the 125 µm electrode compared to the 50 µm electrode, as expected due to its larger surface area.

A figure for comparison between conditions was calculated by averaging the steady state WE current over 5 s, starting from 15 s after the potential step. Chronoamperometry recordings in air-saturated solutions showed that presence of the Nafion membrane slightly lowered the steady-state currents recorded at the WE, but did not eliminate them (Fig. 7B, red bars). The equivalent difference in current density for the 50 µm device was 10.7 Am^{-2} (bare) and 7.14 Am^{-2} (Nafion), and in the
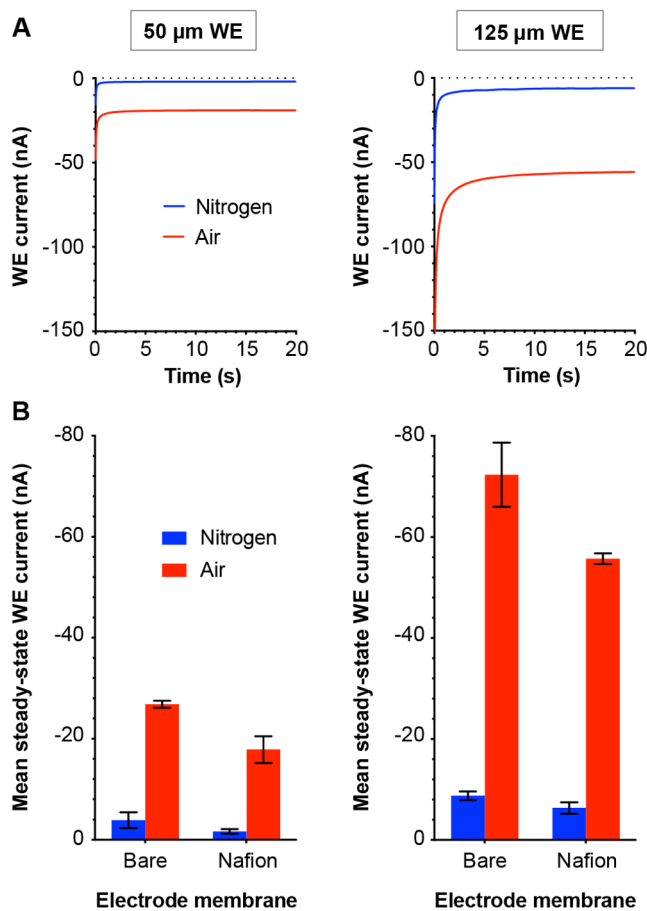
Fig. 7. Chronoamperometry of test electrodes in aqueous solutions saturated with air or purged with nitrogen. A: Typical chronoamperograms from Nafion coated test electrodes. B: Steady state currents from bare or Nafion covered electrodes in solutions saturated with air of purged of oxygen with N_2. Currents were averaged over 15-20 s after the potential step to -0.7 V (vs Ag/AgCl), n = 3 devices for each condition, error bars represent standard error of the mean.

125 μm device was 4.63 Am^{-2} (bare) and 3.57 Am^{-2} (Nafion). This indicates that the annealed and patterned Nafion membrane covering the test electrodes is both permeable to oxygen, and capable of effectively supporting its electrochemical reduction. Interestingly, it has been shown by others that deposition of Nafion onto a platinum electrode causes 15-20% of the surface area to be blocked for electrochemical reactions [17], likely because only sections in contact with the hydrated Nafion nanochannels will be active. This effect may explain the decreased current density we observed at the Nafion coated electrodes. The greater current densities observed in the 50 μm devices compared to the 125 μm devices is due to the known increase in mass transport efficiency at microelectrodes as electrode size is decreased [18].

To confirm that the test electrodes were selectively detecting oxygen, and explore the utility of the Nafion/test electrode system as a sensor, the same measurements were repeated in solutions purged of oxygen by bubbling with nitrogen. Significantly lower currents were recorded from both the bare

and Nafion covered test electrodes in nitrogen purged solutions (Fig. 7B, blue bars). This indicates that the system is selectively reporting the electrochemical reactions of oxygen at the electrodes surfaces, and that Nafion shows promise as a solid electrolyte layer for an oxygen sensor. In addition, both the 50 and 125 μm test electrodes provided usable measurements, providing proof-of-principle for miniaturization of the system.

VI. CONCLUSIONS

Test structures for assessing the performance of a Nafion solid electrolyte membrane were designed and fabricated. These structures provided quantitative information to support optimization of the Nafion design and patterning process, as well as evaluation of its performance parameters.

Specifically, we found that use of AZ726 photoresist developer during processing led to damage of the Nafion structures, which correlated with impaired durability under simulated conditions of use. In contrast, MF-26A developer did not cause visible damage and a diluted solution of MF-26A was associated with the highest durability, so is therefore optimal for Nafion processing. The surface that allowed greatest Nafion durability was PECVD silicon dioxide, indicating that this material should be used as a top passivation layer in the sensor. In addition, the excellent durability obtained on Pt suggests Nafion will not be adversely affected by the presence of underlying electrodes. The functional differences in durability with underlying material were not matched by changes in scratch test critical load. This suggests that scratch tests cannot be used as an indication of lifetime in PBS.

Using a set of test electrodes covered with a patterned Nafion membrane, the Nafion was shown to be oxygen permeable and able to support the electrochemical reduction of oxygen at an electrode surface. This indicates that Nafion can act as an effective electrolyte, and provides proof-of-concept that it would be suitable for use in a miniaturized solid-state implantable oxygen sensor in biomedical applications.

REFERENCES

[1] S. R. McKeown, "Defining normoxia, physoxia and hypoxia in tumours—implications for treatment response," *The British Journal of Radiology,* vol. 87, no. 1035, 2014.

[2] P. Le Roux, "Physiological Monitoring of the Severe Traumatic Brain Injury Patient in the Intensive Care Unit," *Current Neurology and Neuroscience Reports,* vol. 13, no. 3, 2013.

[3] T. Parker, D. Brealey, A. Dyson, and M. Singer, "Optimising organ perfusion in the high-risk surgical and critical care patient: a narrative review," *British Journal of Anaesthesia,* vol. 123, no. 2, pp. 170-176, 2019.

[4] E. Roussakis, Z. Li, A. J. Nichols, and C. L. Evans, "Oxygen-Sensing Methods in Biomedicine from the Macroscale to the Microscale," *Angewandte Chemie International Edition,* vol. 54, no. 29, pp. 8340-8362, 2015.

[5]   L. C. Clark, "Monitor and control of blood and tissue oxygen tension," *Transactions - American Society for Artificial Internal Organs,* vol. 2, pp. 41-48, 1956.

[6]   A. Kusoglu and A. Z. Weber, "New Insights into Perfluorinated Sulfonic-Acid lonomers," *Chemical Reviews,* vol. 117, no. 3, pp. 987-1104, 2017.

[7]   H.-j. Lee, H.-M. Kim, J.-H. Park, and S.-K. Lee, "Fabrication and characterization of micro dissolved oxygen sensor activated on demand using electrolysis," *Sensors and Actuators B: Chemical,* vol. 241, pp. 923-930, 2017.

[8]   W. P. Chan *et al.*, "A Monolithically Integrated Pressure/Oxygen/Temperature Sensing SoC for Multimodality Intracranial Neuromonitoring," *Ieee Journal of Solid-State Circuits,* vol. 49, no. 11, pp. 2449-2461, 2014.

[9]   P. Wang, Y. Liu, H. D. Abruna, J. A. Spector, and W. L. Olbricht, "Micromachined dissolved oxygen sensor based on solid polymer electrolyte," *Sensors and Actuators B-Chemical,* vol. 153, no. 1, pp. 145-151, 2011.

[10]   G. W. McLaughlin, K. Braden, B. Franc, and G. T. A. Kovacs, "Microfabricated solid-state dissolved oxygen sensor," *Sensors and Actuators B-Chemical,* vol. 83, no. 1-3, pp. 138-148, 2002.

[11]   J. R. K. Marland *et al.*, "Test structures for optimizing polymer electrolyte performance in a microfabricated electrochemical oxygen sensor," *2017 International Conference of Microelectronic Test Structures (ICMTS),* pp. 1-5, 2017.

[12]   L. A. Zook and J. Leddy, "Density and solubility of nafion: Recast, annealed, and commercial films," *Analytical Chemistry,* vol. 68, no. 21, pp. 3793-3796, 1996.

[13]   D. B. Hall, P. Underhill, and J. M. Torkelson, "Spin coating of thin and ultrathin polymer films," *Polymer Engineering & Science,* vol. 38, no. 12, pp. 2039-2045, 1998.

[14]   M. Šulc *et al.*, "Nanoscratch test — A tool for evaluation of cohesive and adhesive properties of thin films and coatings," *EPJ Web of Conferences,* vol. 48, no. 00027, pp. 1-4, 2013.

[15]   S. J. Bull and E. G. Berasetegui, "An overview of the potential of quantitative coating adhesion measurement by scratch testing," *Tribology International,* vol. 39, no. 2, pp. 99-114, 2006.

[16]   H. F. M. Mohamed, S. Kuroda, Y. Kobayashi, N. Oshima, R. Suzuki, and A. Ohira, "Possible presence of hydrophilic SO3H nanoclusters on the surface of dry ultrathin Nafion® films: a positron annihilation study," *Phys. Chem. Chem. Phys.,* vol. 15, no. 5, pp. 1518-1525, 2013.

[17]   S. K. Zecevic, J. S. Wainright, M. H. Litt, S. L. Gojkovic, and R. F. Savinell, "Kinetics of O2 reduction on a Pt electrode covered with a thin film of solid polymer electrolyte," *Journal of the Electrochemical Society,* vol. 144, no. 9, pp. 2973-2982, 1997.

[18]   K. Stulík, C. Amatore, K. Holub, V. Marecek, and W. Kutner, "Microelectrodes. Definitions, characterization, and applications (Technical report)," *Pure and Applied Chemistry,* vol. 72, no. 8, pp. 1483-92, 2000.